Microchemical Journal 209 (2025) 112647

Contents lists available at ScienceDirect

Microchemical Journal

journal homepage: www.elsevier.com/locate/microc

Ultrasound-assisted protein-enhanced graphene synthesis for rapid electrochemical antibody sensing

Ana R. Cardoso [a,b], A. Suleimenova [a,b], João Frederico Alves [a], Manuela F. Frasco [a], Pedro Barquinha [b], M. Goreti F. Sales [a,*]

[a] BioMark, CEMMPRE, ARISE, Department of Chemical Engineering, Faculty of Sciences and Technology, University of Coimbra, Coimbra, Portugal
[b] CENIMAT-i3N, Department of Materials Science, NOVA School of Science and Technology, NOVA University Lisbon and CEMOP/UNINOVA, Caparica, Portugal

ARTICLE INFO

Keywords:
Graphene
Carbon-working electrode
SARS-CoV-2
Spike protein
Electrochemical biosensor
Point-of-care testing

ABSTRACT

This study presents a novel method for the fabrication of graphene as a functional interface for electrochemical sensors. Graphene was synthesized by probe-assisted ultrasonic exfoliation of graphite stabilized by the SARS-CoV-2 spike (S) protein. In this dual-function approach, the S protein is used for both graphene stabilization and antibody recognition, simplifying the production of biosensors.

The biosensor was fabricated by modifying a carbon working electrode with the stabilized graphene-S-protein complex. Electrochemical impedance spectroscopy revealed a linear detection range from 1.0 pg/mL to 10.0 ng/mL in diluted human serum, with a detection limit of 0.17 pg/mL. The high selectivity for the S protein was confirmed against the SARS-CoV-2 nucleocapsid protein. The device successfully analysed serum samples, demonstrating its practical application.

These results emphasize a simple, innovative platform that integrates graphene synthesis and biosensor functionality. This approach not only ensures a sensitive and stable substrate for monitoring antibodies against SARS-CoV-2, but also offers an approach that can be extended to detect different antibodies, by selecting the stabilizing protein that binds to the intended antibody.

1. Introduction

Graphene-based electrochemical biosensors enable the sensitive and cost-effective detection of various biomolecules due to the excellent properties of graphene sheets, which are electrically conductive, have a large surface area and excellent dispersibility, and can be easily functionalized [1–4]. These physical and chemical properties, combined with low production costs and low environmental impact, make graphene an extremely attractive material for biosensing applications [5–8].

Graphene can be obtained by a variety of methods [9]. Bottom-up strategies rely on the chemical arrangement of carbon atoms to form graphene layers, while top-down strategies use a different material as a carbon source to obtain graphene. Mechanical exfoliation of graphite flakes is considered one of the simplest and most cost-effective methods [10]. This includes ultrasonic treatment, which makes it possible to shorten the time for exfoliation and produce graphene sheets of more homogeneous size. With high-power ultrasound, thin and single-layer graphene sheets are usually produced in a few minutes, although damage and defects can occur at the edges of the graphene flakes [11,12].

In the specific case of electrochemical sensor technology, graphene should interact with the sensor surface, which is why it should be present in the form of an aqueous suspension. However, graphene is naturally hydrophobic due to the condensed aromatic benzene rings it contains. This can be modified by specific biofunctionalization that favours the dispersion of graphene nanosheets in an aqueous environment. There are many approaches to this end, including the mechanical exfoliation of graphite in the presence of proteins [13–15]. The shear and turbulence forces of a kitchen blender were formerly used to exfoliate graphite in the presence of various proteins [14]. The tests were carried out with bovine serum albumin (BSA), β-lactoglobulin, ovalbumin, lysozyme and haemoglobin, as these proteins are inexpensive and sourced from the food industry. BSA was the best protein in this study, intercalating into the nanosheets of graphene and thus

* Corresponding author at: Department of Chemical Engineering, Faculty of Sciences and Technology, University of Coimbra, Rua Sílvio Lima, Pólo II, 3030-790 Coimbra, Portugal.
E-mail address: goreti.sales@eq.uc.pt (M.G.F. Sales).

https://doi.org/10.1016/j.microc.2025.112647
Received 9 October 2024; Received in revised form 30 December 2024; Accepted 1 January 2025
Available online 2 January 2025

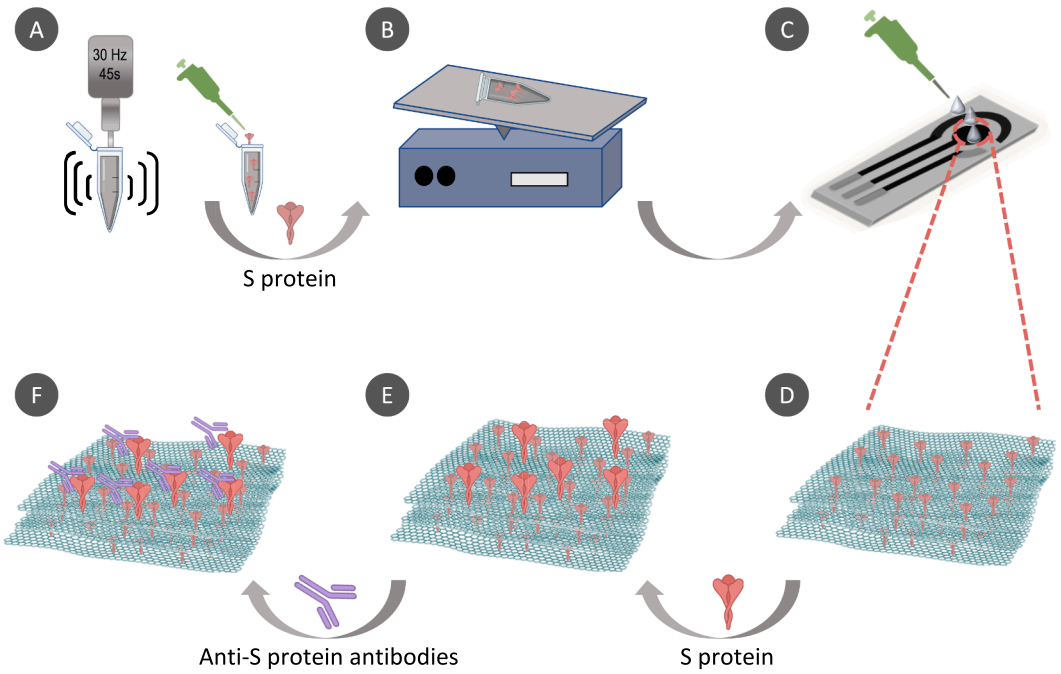

Fig. 1. Schematic representation of biosensor construction: (A) ultrasonic exfoliation of graphite; (B) biofunctionalization of graphene sheets with spike (S) protein; (C, D) modification of the surface of the working electrode with the S protein biofunctionalized graphene; (E) addition of S protein as recognition element; (F) detection of antibodies to SARS-CoV-2.

contributing to the stabilization of the graphene sheets.

Although the addition of BSA was a successful way to produce the graphene nanosheets cheaply and in less than an hour, this time frame could be shortened to a few minutes/seconds if a high-power ultrasound was used. The resulting graphene suspension is expected to be stable, which can be achieved by adding a suitable protein that can also be used for sensing purposes. This would be the case if the protein used was an antigen for a specific antibody. Although any antibody/antigen pair would be suitable for this principle, the proof of concept for this idea was tested with protein S (spike protein of SARS-CoV-2) and its antibody to monitor the immunological response against this viral infection.

There are currently several electrochemical biosensors in the literature for the detection of SARS-CoV-2 antibodies. These include the use of electrochemical impedance spectroscopy (EIS) and cyclic voltammetry (CV), which contain interdigitated electrodes [16] or complex chemistry to ensure accurate capture of antibodies [17,18]. Overall, these approaches are associated with complex biosensing designs that hardly reach the end user in commercial applications. Whilst the simplicity of the biosensor design is the key element for any intended commercial application, sensitivity and selectivity must be ensured, and these are linked to the specific materials used [19–22], with graphene being employed to improve sensitivity. It offers high mechanical strength, thermal stability (which can have a positive impact on reproducibility) and a large surface area (important for immobilization) while improving electron transfer at room temperature [23,24].

Therefore, the green production of graphene containing the SARS-CoV-2 S protein as a stabilizing and recognising element is reported here (Fig. 1). The optimization of graphene production and the design of the biosensor are described. The best conditions were employed for testing human serum samples. The general characterization of the biosensor confirms its usefulness in the analysis of serum for its antibody content against SARS-CoV-2.

2. Experimental section

2.1. Apparatus

The exfoliation of graphite was performed in a VCX 750 ultrasonic processor (Sonics & Materials, Inc, USA) and the stabilization of the resulting graphene nanosheets with spike (S) protein was carried out in an MB-101 mixing block (Bioer, China). The main electrochemical experiments were performed on screen-printed carbon electrodes (C-SPEs) (DRP-110; Metrohm Dropsens, Spain) containing a working electrode (WE) and an auxiliary electrode made of carbon and a reference electrode made of silver. This three-electrode system was connected to a PalmSens4 potentiostat/galvanostat controlled by PSTrace v5.9 software (PalmSens BV, Netherlands). Scanning electron microscopy (SEM) images were acquired using an FEI Quanta 400 FEG ESEM device. Raman analysis was made in an InVia™ confocal Raman microscope Renishaw RE04 with a 532 nm, 50 mW laser used at 5 % and 10 % power, calibration with Silicon standard and spectra taken from 300 to 3200 cm^{-1}.

2.2. Reagents and solutions

Potassium hexacyanoferrate (II) 3-hydrate ($K_4[Fe(CN)_6].3H_2O$) was acquired from Panreac and potassium ferricyanide (III) ($K_3[Fe(CN)_6]$) was obtained from Carlo Erba. Potassium chloride (KCl) and isopropanol (70 %) were obtained from Fluka/Honeywell. Phosphate buffered saline (PBS) tablets, graphite, and dimethyl sulfoxide (DMSO) were purchased from Sigma-Aldrich. Nafion® (20 wt% in alcohols) was acquired from Quintech. Cormay Serum HN was acquired from PZ Cormay S.A. The recombinant SARS-CoV-2 S protein (S1 subunit derived from *E. coli*) and the polyclonal Rabbit anti-SARS-CoV-2 S1F antibody were procured from RayBiotech. All chemicals were of analytical grade and ultrapure laboratory grade water was used (conductivity <0.1 μS/cm).

2.3. Production of biofunctionalized graphene

The mechanical exfoliation of graphite was performed in a high-

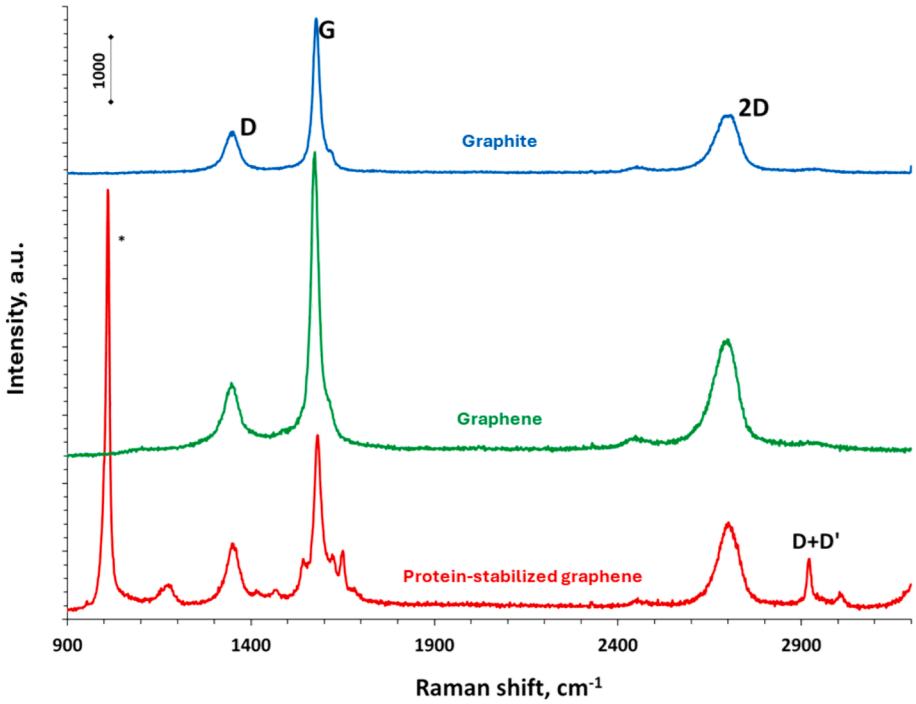

Fig. 2. Raman spectra of the graphite material before ultrasonication, the exfoliated graphite after sonication (named as graphene) and the intercalation of the exfoliated graphene sheets with S protein (named as protein-stabilized graphene), all casted on a glass substrate, highlighting the most relevant peaks.

energy ultrasonic probe at an amplitude of 30 % for 45 s in a solution containing 5 mg of graphite flakes in 1 mL of ultrapure water and DMSO (ratio 2:8), in a similar procedure to that described in [25]. Then, 10 μL of a Nafion® solution diluted in isopropanol (ratio 1:3) was added to improved binding of the graphene sheets upon deposition on the electrode [26]. A volume of 100 μL of a 2×10^{-6} mol/L solution of SARS-CoV-2 S protein was added to this mixture and homogenized/dispersed in a mixing block at room temperature for 2 h to obtain the S protein biofunctionalized graphene. The operating frequency was varied between 25 and 30 KHz and the exfoliation time between 45 and 120 s [27].

2.4. Electrochemical measurements and procedures

All electrochemical measurements were performed at room temperature. First, the surface of the WE was cleaned by an electrochemical CV treatment in which a potential of −1.0 V to +1.0 V was applied with a potential step of 0.01 V and a scan-rate of 0.05 V/s in 0.1 M KCl diluted in ultrapure water. A 5.0 mmol/L ferri/ferrocyanide redox probe solution in 10 mL of PBS (0.010 mol/L, pH 7.4) was used as the electrolyte. EIS was performed in open circuit with a sinusoidal potential perturbation with an amplitude of 0.01 V and 50 data points logarithmically distributed over a frequency range of 0.1–100,000 Hz. Square wave voltammetry (SWV) method operated from −0.3 to +0.7 V, with a frequency of 2 Hz and a step height of up to 2.5 mV. The evaluation of the KCl effect on the electrochemical behaviour of the C-SPE was determined by EIS and SWV measurements, evaluating the impact upon the charge transfer resistance (R_{ct}) and current values, when compared to the unmodified C-SPE.

Protein-stabilized graphene was drop-casted (15 μL) on the WE of the cleaned C-SPE and dried at 40 °C for 150 min. Then, the surface of the WE was further incubated with 2×10^{-6} mol/L S protein prepared in PBS buffer at room temperature for 60 min. The electrochemical behaviour of the biosensor after modification with graphene biofunctionalized with S protein and after the subsequent reinforcement with S protein were monitored by EIS and SWV. Stabilization of biosensor was followed by EIS readings, after consecutive buffer incubations, until the R_{ct} values remained unchanged.

2.5. Analytical performance

The analytical performance was first studied in PBS buffer (0.010 mol/L, pH 7.4). The biosensor was incubated in PBS at room temperature for 30 min until it stabilized. Then, the calibration curve was established by incubating the biosensor with increasing concentrations (1.0 pg/mL, 10.0 pg/mL, 100.0 pg/mL, 1.0 ng/mL, 10.0 ng/mL, 100.0 ng/mL) of SARS-CoV-2 S protein antibody prepared in PBS buffer, at room temperature for 30 min. A similar calibration was tested in C-SPEs modified with nonfunctionalized graphene and with graphene without the additional S protein recognition layer. These served as controls to compare the electrochemical behaviour under the different conditions.

A more complex matrix was then tested, and the analytical performance of the biosensor was evaluated in 1000-fold diluted human serum. The biosensor was first stabilized with the diluted serum for 30 min at room temperature. Then, the increasing concentrations (1 pg/mL to 100 ng/mL) of SARS-CoV-2 S protein antibody prepared in diluted human serum were also incubated in the biosensor for 30 min at room temperature. Selectivity assays were performed by testing the response of the biosensor in a solution containing a mixture of anti-S antibody and anti-nucleocapsid (N) antibody, both at a concentration of 10 pg/mL in PBS buffer. Each condition was evaluated after incubation of the biosensor for 30 min at room temperature. All electrochemical measurements were based on EIS by determining the variations in R_{ct} values.

3. Results and discussion

3.1. Graphene production by protein-assisted ultrasonication

Direct ultrasonic exfoliation of graphite in liquid is one route to obtain graphene from bulk graphite [28] due to the energy input to the graphite in liquid media via the sonication and the contribution from the selected solvent in decreasing the potential energy between adjacent layers in the bulk graphite (to overcome the weak out-of-plane van der Waals interactions between these layers). In this study, a probe

Table 1
List of the Raman shifts of the main peaks observed in the Raman spectra for the different materials and ratio of the intensities of G/D and 2D/G peaks.

Material	Raman shift of the peak (cm^{-1})			Intensity peak ratio	
	D	*G*	*2D*	$I_{G/D}$	I_{2D}/I_G
Graphite	1351.7	1577.8	2709.9	3.76	0.37
Graphene	1350.2	1574.7	2701.6	4.61	0.31
Protein-stabilized Graphene	1351.9	1581.2	2698.8	2.73	0.61
SPE (carbon electrode)	1360.3	1581.2	2714.2	1.32	0.23
Protein-stabilized Graphene-SPE	1353.6	1581.2	2708.6	5.10	0.38

sonication was employed, optimizing the main parameters to contribute to the formation of high conductivity (bio)graphene material. The operating frequency was tested and 30 KHz were find sufficient to produce graphene sheets without significant degradation of the materials. The time was optimized with the purpose of having a homogenous dispersion of exfoliated graphene sheets that enhanced the electrochemical conductivity features of the carbon WE on the SPE. Ultrasound irradiation was tested from 45 to 120 s, and the best electrochemical features were obtained for 45 s (Fig. S1). Longer periods promoted an excessive oxidation of the material. The solvent employed was DMSO, due to the need of a compatible solvent between the exfoliation stage made by sonication [29] and the subsequent mixing with a protein material that is supposed to keep the original tertiary structure of the protein and intercalate with the graphene sheets to avoid their aggregation.

The Raman spectrum of graphite evidenced the typical D, G and 2D bands (Fig. 2), which are in agreement with the typical Raman shifts of the pristine graphite [30]. The subsequent exfoliation of graphite (herein named as graphene) yielded a significant increase of the G band; the G band is recognized as the graphene characterizing band, corresponding to stretching mode of C-C bond of sp^2 carbons hybridization. In turn, the D band decreased significantly. This band is known as a defect-activated band corresponding to the presence of carbon atoms with sp^3 hybridization, typically at the edges of graphene sheets. The 2D band was present in both spectra with good symmetry, suggesting good stacking of graphene layers from the raw material graphite, with minimum disruption of graphite stacking order [31]. This 2D band is an overtone of D band, appearing from 2 phonon graphene lattice vibrations, a second order two photon process. Overall, Raman spectra confirmed the appearance of graphene sheets, due to the significant increase of the G/D peak ratio (Table 1) after exfoliation of graphite by ultrasound.

The presence of S protein in between the graphene sheets was considered essential. Alone, graphene sheets would tend to keep π–π stacking/van der Walls interactions between the aromatic carbon rings, which would favour the coalescence of the sheets. By adding the S protein, the protein molecules act as obstacles to this coalescence, because their hydrophilic regions confer them easy mobility throughout the aqueous suspension, enabling their intercalation in between the graphene sheets and subsequent stabilization of the suspension via protein–graphene interactions [32,33]. In terms of Raman spectra, the presence of S protein yielded a more complex spectrum, from which D, G and 2D peaks remained evident, although their relative intensities changed significantly [33,34]. The G/D peak ratio changed to lower values than graphite, due to the formation of a composite material with graphene, also containing various functional groups that generated various additional Raman peaks. Comparison of peak shape and fit curve to data provided by Ferrari et al. [35] studying 2D peak as a function of graphene layer numbers, data suggest that the protein-stabilized graphene had a 3–4 layered structure. This graphene material also had a D + D' band at 2921 cm^{-1} that is sometimes identified as D + G, being present in defective graphene structures [35]. The presence of graphene defects showed a higher electron transfer rate on graphene edge-plane than in basal plane that could be beneficial for the electrochemical measurements and analytical performance of a developed biosensor [36,37].

3.2. Biosensor assembly and characterization

The assembly of the biosensor included an initial surface treatment with KCl to remove impurities that could be present in the pristine C-SPEs. Then, ultrasonically exfoliated graphite biofunctionalized with S protein was drop-casted on the WE. To ensure higher antibody recognition capacity in the system, the amount of S protein was increased by casting a new solution of S protein on the surface of the WE. The electrochemical response to the different steps of biosensor assembly was monitored by EIS (Fig. 3A, B) and SWV (Fig. 3C, D).

The electrochemical cleaning procedure with KCl redox cycles resulted in a decrease in R_{ct} values from about 1093 Ω to 419 Ω (Fig. 3B) and an increase in the current from 34.73 μA in the pristine state to 56.09 μA, as observed by SWV measurements (Fig. 3D). This procedure reduced the potential difference between the peaks of oxidation and reduction, enhancing the conductivity of the surface and decreasing variability between electrodes, which positively and directly affects the reproducibility of this work. The addition of protein-stabilized graphene had a double-edged effect, since graphene nanosheets have a very well described ability to increase conductivity in three-electrode systems [20,21], but the presence of the S protein distributed between its sheets increased the R_{ct} from 419 Ω to 743 Ω (Fig. 3B) and decreased de current from 56.09 μA to 30.77 μA (Fig. 3D). The last phase of biosensor assembly consisted in reinforcing the immobilization of the S protein biorecognition element, with its binding being confirmed by the significant increase in the R_{ct} to 1046 Ω (Fig. 3B) and decrease in current to 18.39 μA (Fig. 3D). The obtained results were as expected due to the large recognition protein that hinders electron transfer on the modified surface of the WE.

The repeatability of the fabricated sensor has been thoroughly evaluated, through repeated measurements of the blank. The average values were of 1218 Ω and the relative standard deviations of the blank were ~6%, thereby confirming the good repeatability of the response.

The electrode surface modified with biofunctionalized graphene was analysed by SEM (Fig. 3, bottom), and compared to a bare SPE electrode. Although the magnification of the SEM images is little, the presence of graphene sheets is evidenced when comparing Fig. 3G and J. Another image of the graphene sheets has been added to the Supplementary section (Fig. S2), where the graphene sheets are more evident. The presence of graphene is consistent with the brighter light obtained in part of some of material deposited on the bare SPE. This brightness can be attributed to the increased conductivity linked to the morphology of the graphene sheets. These results are further consistent with the EIS data, because the addition of graphene sheets alone resulted in a decrease in Rct, indicating improved electron transfer efficiency due to the conductive properties of graphene.

3.3. Analytical performance of the biosensor

The biosensor responded to a range of increasing concentrations of S protein antibody diluted in PBS (1 pg/mL to 100 ng/mL), as shown in the Nyquist plots of the EIS measurements (Fig. 4A). This response was evaluated in three replicates, and a linear trend was obtained from 1 pg/mL to 10 ng/mL. R_{ct} values versus the logarithm of antibody concentration showed a slope of 158.07 Ω/decade and a squared correlation coefficient of 0.994 (Fig. 4B). At the concentration of 100 ng/mL, the saturation of the sensor may explain the lack of response. The replicates were highly reproducible, with RSD values ranging from 4 % (minimum) to 11 % (maximum), and a limit of detection (LOD) of 0.08 pg/mL was obtained.

The long-term stability of the sensors was tested over a period of 10 days, by preparing multiple units without any chemical/physical

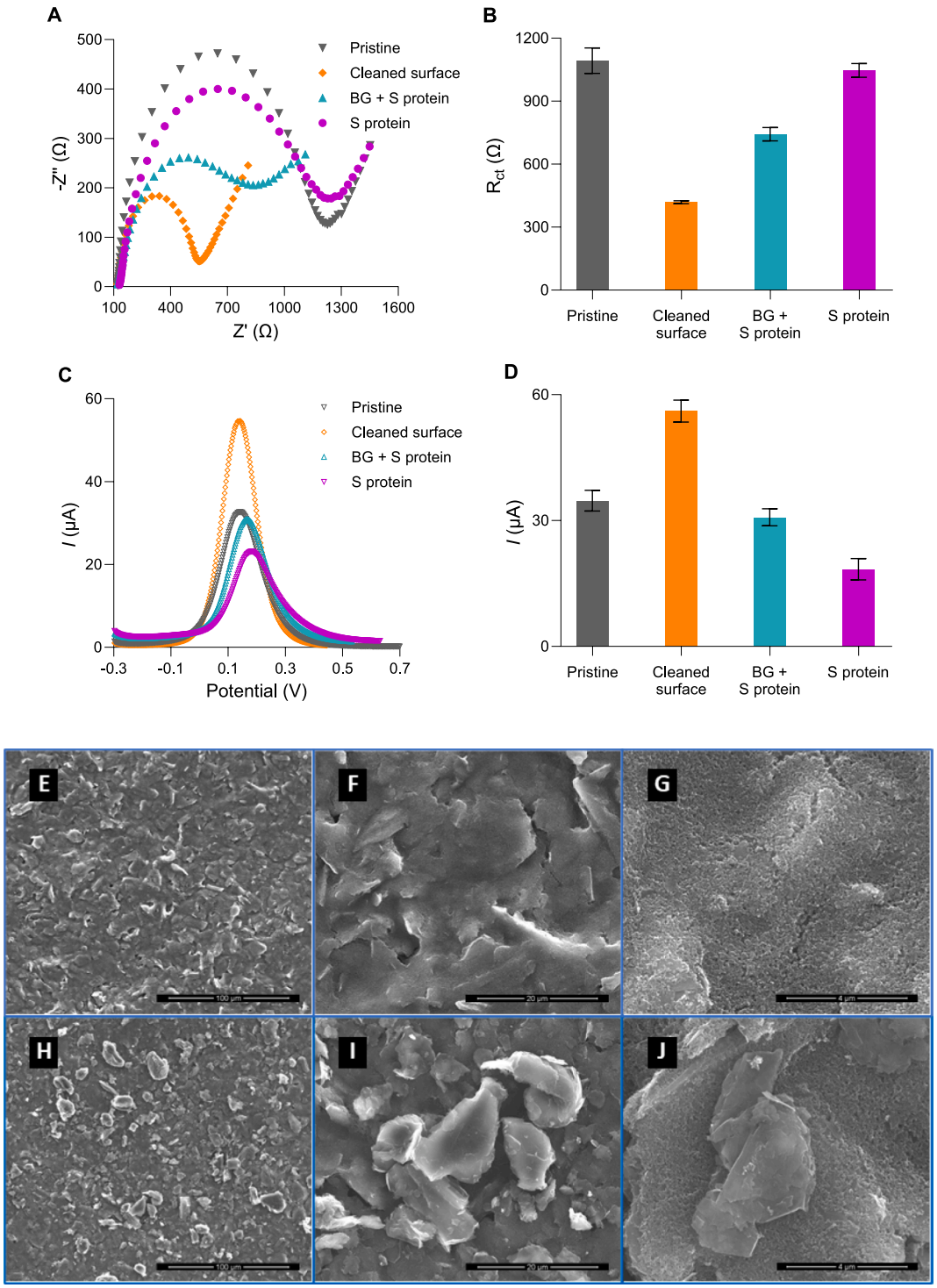

Fig. 3. Electrochemical data (plots) collected with the iron redox probe prepared in PBS buffer, during biosensor construction, corresponding to EIS – (A) Nyquist plots/(B) average R_{ct} values – and SWV – (C) voltammograms/(D) average current peaks intensities. Data includes pristine C-SPEs, after cleaning, after modification with graphene functionalized with S protein and exfoliated in 45 s, and after adding S protein as biorecognition element. SEM images of the WE of pristine C-SPE (E–G) and after modification with the protein-stabilized graphene (H–J).

procedure that could improve stability, keeping them stored in the fridge, under a humid environment. Two units were calibrated at day 3 and other two at day 5. In day 3, a consistent linear response was observed from 10 pg/ml to 100 ng/ml, with an average slope of 155.7 (±19.2) Ω/decade concentration (Fig. S3). On day 5, the impedance spectra showed a second semicircle, indicating the appearance of a heterogeneous surface, probably due to the partial denaturation of the proteins and their interaction with the graphene layer (Fig. S4). Overall, this meant that each sensing unit could be calibrated after 3-days of preparation, with negligible change in the analytical behaviour, and that it would be relevant to establish additional procedures to improve the stability of the antibodies attached to the electrode.

To evaluate the response of the electrochemical biosensor in a more realistic situation, diluted human serum was used, which has a complex composition of potentially interfering species. Increasing concentrations (1 pg/mL to 100 ng/mL) of the anti-S protein antibody diluted in human

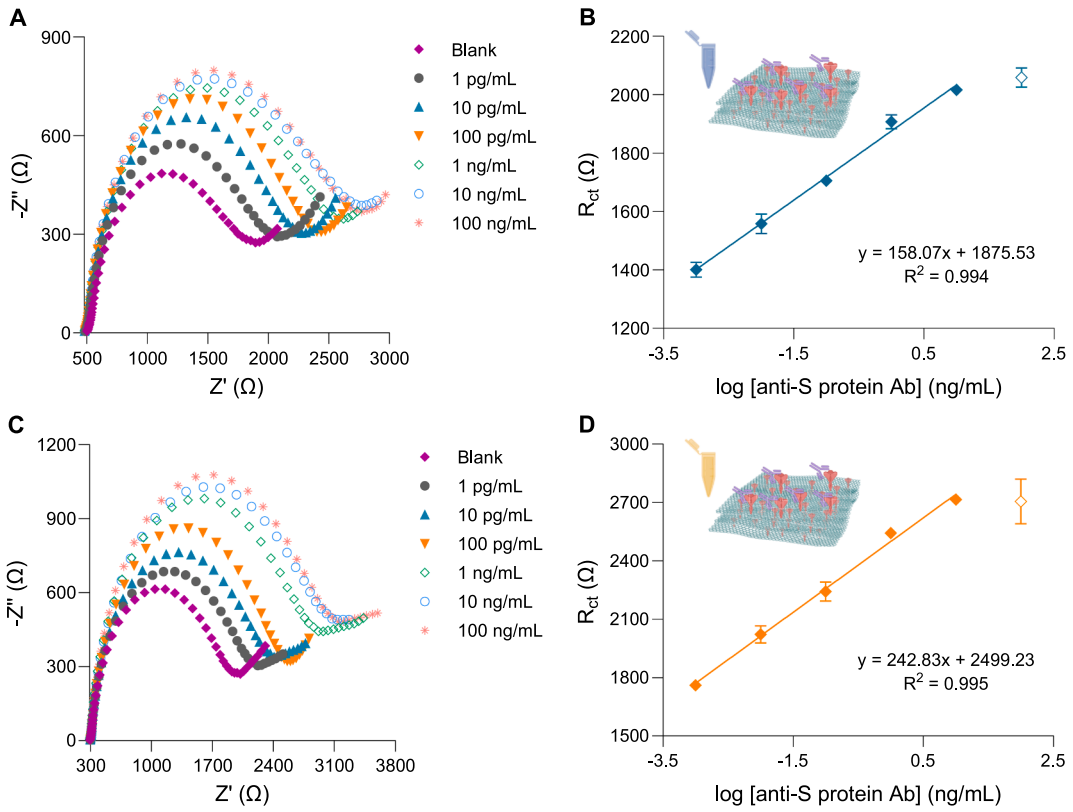

Fig. 4. Nyquist plots (A,C) and the average calibration curves (B,D) of the optimized biosensors, obtained by consecutive incubation of standard solutions of anti-spike protein antibodies prepared in PBS buffer (A,B) or in diluted human serum (C,D). Readings are obtained with the iron redox probe, prepared in PBS buffer.

serum were tested, as shown in the Nyquist plots of the EIS measurements (Fig. 4C). This calibration (three replicates) showed similar behavior to the results obtained in PBS buffer. Here, there was a linear trend for the R_{ct} values against the anti-S protein antibody standards (up to 10 ng/mL) prepared in diluted human serum, with a slope of 242.83 Ω/decade and a squared correlation coefficient of 0.995 (Fig. 4D), and LOD of 0.17 pg/mL. As expected, the LOD was higher in serum than in buffer due to the more complex serum matrix, which presents higher ionic composition and additional difficulties in detecting the biomolecule of interest.

The aim of designing the biosensor with an additional S protein layer was to increase the sensitivity. This was confirmed by comparing the performance of the biosensor with C-SPEs prepared with graphene without biofunctionalization, and with or without the additional S protein layer. The C-SPE whose WE was modified with graphene without biofunctionalization did not show a linear response to increasing concentrations of SARS-CoV-2 S protein antibody diluted in PBS (1 pg/mL to 10 ng/mL) (Fig. S5A, B). Regarding the electrode modified with protein-stabilized graphene, the response shows a more intense tendency for a linear behaviour in the same concentration range (1 pg/mL to 10 ng/mL), although not statistically relevant (Fig. S5C, D). Besides the low-quality correlation coefficient, the slope was lower (68.19 Ω/decade) than that obtained in the final biosensor tested in PBS buffer (158.07 Ω/decade). These results suggest that the addition of S protein after graphene on the surface of the WE was a crucial step to guarantee a highly sensitive biosensor.

There are few reports of electrochemical biosensors based on C-SPEs whose surface was modified with carbon nanomaterials to detect anti-S protein antibodies. In one study, a functional substrate was prepared by electrodeposition of graphene quantum dots and polyhydroxybutyric acid. The voltametric signal was followed and showed a correlation between 100 ng/mL and 10 μg/mL anti-S antibodies, and a LOD of 100 ng/mL was obtained [38]. In another approach, a carbon electrode was modified with reduced graphene oxide in combination with a specific binding peptide and a LOD of 0.77 μg/mL was determined [39]. Other carbon nanomaterials such as carboxylated single-walled carbon nanotubes have also been investigated for the development of electrochemical biosensors to detect antibodies against SARS-CoV-2 [18]. The impedimetric properties of the biosensor followed by EIS displayed a linear response between 1 pg/mL and 10 ng/mL, with a LOD of approximately 0.7 pg/mL [18]. Thus, among the studies that have used carbon nanomaterials, the current approach is a simple and

Table 2
Relevant papers using graphene nanomaterials and electrochemical methods for monitoring antibodies against of SARS-CoV-2 via protein S binding.

Assembly details	Linear Range	LOD	Reference
Carbon SPE modified with SWCNT, activated with EDAC/NHS, functionalized with *p*-phenylenediamine. The SARS-CoV-2 Spike protein was then immobilized.	1.0 pg/mL to 10 ng/mL	0.7 pg/mL	[18]
GQD and PHB to create a functional surface for anchoring RBD of S Protein.	100 ng/mL to 10 μg/mL	100 ng/mL	[38]
Peptide and rGO mixture were immobilized on the WE of the carbon SPE.	0.3 to 5.2 μg/mL	0.77 μg/mL	[39]
Graphene was synthesised by ultrasonic exfoliation of graphite stabilized by the SARS-CoV-2 Spike protein and immobilized on the carbon SPE.	1.0 pg/mL to 10 ng/mL	0.17 pg/mL	This work

SPE: Screen-Printed Electrode; **SWCNT:** Carboxylated single-walled carbon nanotubes; **EDAC/NHS:** *N*-ethyl-*N*′-(3-dimethylaminopropyl) carbodiimide hydrochloride/*N*-hydroxysuccinimide; **SARS-CoV-2:** Severe Acute Respiratory Syndrome Coronavirus 2; **GQD:** Graphene Quantum Dots; **PHB:** Polyhydroxybutyric acid; **RBD**: Recognition site receptor-binding domain; **rGO**: reduced graphene oxide; **WE:** Working Electrode.

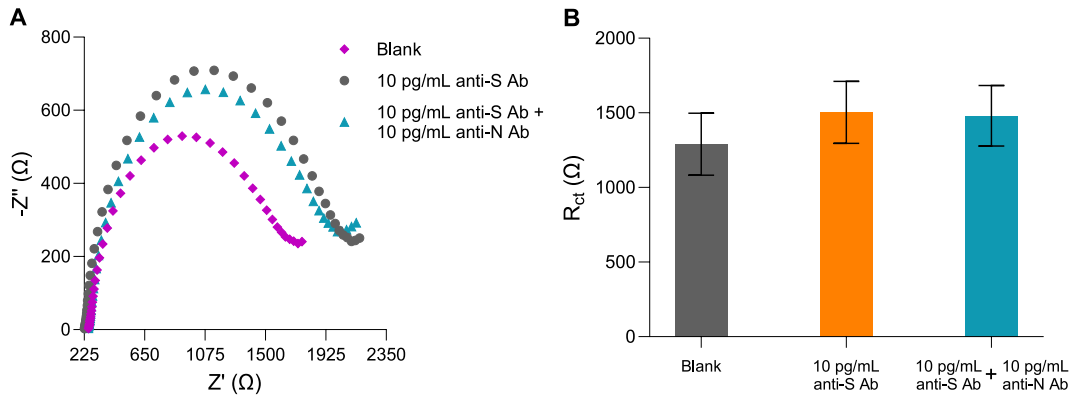

Fig. 5. Nyquist plot (A) of the optimized biosensor incubated in blank solution, anti-spike (S) protein antibody (10 pg/mL) and anti-spike (S) protein antibody (10 pg/mL) with anti-nucleocapsid (N) protein antibody (10 pg/mL), and the average data with independent biosensors in bar plot (B). Readings are obtained with the iron redox probe, prepared in PBS buffer.

straightforward approach, capable of generating accurate data by measuring very low concentrations of SARS-CoV-2 spike antibodies in complex samples, achieving even lower LOD than previous studies in the literature (Table 2).

3.4. Selectivity assays

To determine the ability of the biosensor to selectivity detect SARS-CoV-2 S protein antibodies in samples containing multiple compounds, it is necessary to evaluate its response to interfering species. SARS-CoV-2 anti-N antibodies, which are commonly found in the serum of SARS-CoV-2 infected patients, were selected to study their effect on biosensor response. To attain this, a concentration (10 pg/mL) of SARS-CoV-2 anti-N antibodies and the same concentration of a solution containing a mixture of anti-S and anti-N antibodies were tested. Fig. 5A shows the Nyquist plots of the carbon electrodes modified with protein-stabilized graphene, evaluated under these conditions. The average percentage deviation upon the direct readings of anti-S protein antibody produced by anti-N protein antibody was −3.2 % (Fig. 5B). Overall, these results confirmed that anti-N protein antibody had a negligible interfering effect upon the anti-S protein antibody response and that the device was selective in the presence of other antibodies.

3.5. Analytical application

As a proof-of-concept, the device was applied to the detection of anti-S protein antibody in real samples. The first stage of sample analysis was proceeded by a previous calibration in an independent sensor. As sample and standards should be well-tuned, the standard solutions were prepared in buffer. Comparing to the previous calibrations using standard solutions prepared in electrolyte, it was clear that the use of serum samples had no relevant impact on the biosensor response. Using the calibration curve in buffer, the concentrations obtained from S protein in samples in buffer yielded errors ranging from 4 % to 11 %, in different concentration levels.

4. Conclusions

An innovative electrochemical biosensor with high sensitivity for the detection of antibodies against SARS-CoV-2 has been developed. The biosensor utilises a cost-effective technology in which graphite is mechanically exfoliated to obtain graphene sheets that are stabilized with SARS-CoV-2 spike protein. This approach simplifies manufacturing, speeds up production and promotes environmental friendliness.

In general, biosensors require modification of the electrode surface to increase conductivity and immobilize biological recognition elements for improved detection sensitivity. With the presented strategy, these improvements can be achieved at low cost compared to the use of precious metals. Electrochemical characterization confirms that the graphene-modified electrode with an additional layer of immobilized spike protein optimally detects anti-S protein antibodies in both buffer and serum samples and achieves a low detection limit with promising selectivity.

The results of the study demonstrate an optimised green strategy to produce protein-enhanced functional graphene substrates that contribute to sustainability in point-of-care settings. In addition, the biosensor outperforms other diagnostic techniques due to its simplicity in production and handling. Its potential for undergoing a scalable production suggests an effective contribution to the control of the spread of SARS-CoV-2, which can also be transferred to other viruses.

CRediT authorship contribution statement

Ana R. Cardoso: Writing – review & editing, Writing – original draft, Visualization, Validation, Methodology, Investigation, Formal analysis. **A. Suleimenova:** Writing – review & editing, Validation, Methodology, Investigation. **João Frederico Alves:** Writing – review & editing, Validation, Methodology, Investigation. **Manuela F. Frasco:** Writing – review & editing, Visualization, Validation. **Pedro Barquinha:** Writing – review & editing, Visualization, Formal analysis. **M. Goreti F. Sales:** Conceptualization, Funding acquisition, Investigation, Project administration, Resources, Supervision, Writing – review & editing.

Declaration of competing interest

The authors declare that they have no known competing financial interests or personal relationships that could have appeared to influence the work reported in this paper.

Acknowledgements

The authors acknowledge funding through project TecniCov (POCI-01-02B7-FEDER-069745), co-funded by FEDER through COMPETE2020 and Lisboa2020. ARC and JFA acknowledge funding from National Foundation for Science and Technology, I.P. (FCT), Portugal through the PhD grants, references SFRH/BD/130107/2017 (COVID/BD/15279/2022) and 2022.13962.BD, respectively. This research is also funded by FEDER funds through COMPETE (Programa Operacional Factores de Competitividade) and national funds through Fundação para a Ciência e a Tecnologia, I.P. (FCT), in the scope of references UID/EMS/00285/2020 (CEMMPRE), LA/P/0112/2020 (ARISE associated laboratory), LA/P/0037/2020 and UIDB/50025/2020. The authors acknowledge Professor Hugo Águas (NOVA FCT) for the Raman Measurements.

Appendix A. Supplementary data

Supplementary data to this article can be found online at https://doi.org/10.1016/j.microc.2025.112647.

Data availability

No data was used for the research described in the article.

References

[1] J. Peña-Bahamonde, H.N. Nguyen, S.K. Fanourakis, D.F. Rodrigues, Recent advances in graphene-based biosensor technology with applications in life sciences, J. Nanobiotechnol. 16 (2018), https://doi.org/10.1186/s12951-018-0400-z.

[2] V. Georgakilas, M. Otyepka, A.B. Bourlinos, V. Chandra, N. Kim, K.C. Kemp, P. Hobza, R. Zboril, K.S. Kim, Functionalization of graphene: Covalent and non-covalent approaches, derivatives and applications, Chem. Rev. 112 (2012) 6156–6214, https://doi.org/10.1021/cr3000412.

[3] C.I.L. Justino, A.R. Gomes, A.C. Freitas, A.C. Duarte, T.A.P. Rocha-Santos, Graphene based sensors and biosensors, TrAC – Trends Anal. Chem. 91 (2017) 53–66, https://doi.org/10.1016/j.trac.2017.04.003.

[4] A.T. Lawal, Progress in utilisation of graphene for electrochemical biosensors, Biosens. Bioelectron. 106 (2018) 149–178, https://doi.org/10.1016/j.bios.2018.01.030.

[5] M. Safari, A. Moghaddam, A. Salehi Moghaddam, M. Absalan, B. Kruppke, H. Ruckdäschel, H.A. Khonakdar, Carbon-based biosensors from graphene family to carbon dots: a viewpoint in cancer detection, Talanta 258 (2023), https://doi.org/10.1016/j.talanta.2023.124399.

[6] A.A. Lahcen, S. Rauf, T. Beduk, C. Durmus, A. Aljedaibi, S. Timur, H.N. Alshareef, A. Amine, O.S. Wolfbeis, K.N. Salama, Electrochemical sensors and biosensors using laser-derived graphene: a comprehensive review, Biosens. Bioelectron. 168 (2020), https://doi.org/10.1016/j.bios.2020.112565.

[7] J. Sengupta, C.M. Hussain, Graphene-based field-effect transistor biosensors for the rapid detection and analysis of viruses: A perspective in view of COVID-19, Carbon Trends 2 (2021) 100011, https://doi.org/10.1016/j.cartre.2020.100011.

[8] Z. Wan, N.T. Nguyen, Y. Gao, Q. Li, Laser induced graphene for biosensors, Sustain. Mater. Technol. 25 (2020), https://doi.org/10.1016/j.susmat.2020.e00205.

[9] Y.V.M. Reddy, J.H. Shin, V.N. Palakollu, B. Sravani, C.H. Choi, K. Park, S.K. Kim, G. Madhavi, J.P. Park, N.P. Shetti, Strategies, advances, and challenges associated with the use of graphene-based nanocomposites for electrochemical biosensors, Adv. Colloids Interface Sci. 304 (2022), https://doi.org/10.1016/j.cis.2022.102664.

[10] H.A. Alhazmi, W. Ahsan, B. Mangla, S. Javed, M.Z. Hassan, M. Asmari, M. Al Bratty, A. Najmi, Graphene-based biosensors for disease theranostics: development, applications, and recent advancements, Nanotechnol. Rev. 11 (2021) 96–116, https://doi.org/10.1515/ntrev-2022-0009.

[11] K. Muthoosamy, S. Manickam, State of the art and recent advances in the ultrasound-assisted synthesis, exfoliation and functionalization of graphene derivatives, Ultrason. Sonochem. 39 (2017) 478–493, https://doi.org/10.1016/j.ultsonch.2017.05.019.

[12] A. Ciesielski, P. Samorì, Graphene via sonication assisted liquid-phase exfoliation, Chem. Soc. Rev. 43 (2014) 381–398, https://doi.org/10.1039/c3cs60217f.

[13] C. Alatzoglou, M. Patila, A. Giannakopoulou, K. Spyrou, F. Yan, W. Li, N. Chalmpes, A.C. Polydera, P. Rudolf, D. Gournis, H. Stamatis, Development of a multi-enzymatic biocatalytic system through immobilization on high quality few-layer bio-graphene, Nanomaterials 13 (2023), https://doi.org/10.3390/nano13010127.

[14] C. V. Kumar, A. Pattammattel, BioGraphene Direct Exfoliation of Graphite in a Kitchen Blender for Enzymology Applications, in: Methods Enzymol, Academic Press Inc., 2016: pp. 225–244. https://doi.org/10.1016/bs.mie.2016.03.009.

[15] A. Pattammattel, C.V. Kumar, Kitchen chemistry 101: multigram production of high quality biographene in a blender with edible proteins, Adv. Funct. Mater. 25 (2015) 7088–7098, https://doi.org/10.1002/adfm.201503247.

[16] M.Z. Rashed, J.A. Kopechek, M.C. Priddy, K.T. Hamorsky, K.E. Palmer, N. Mittal, J. Valdez, J. Flynn, S.J. Williams, Rapid detection of SARS-CoV-2 antibodies using electrochemical impedance-based detector, Biosens. Bioelectron. 171 (2021), https://doi.org/10.1016/j.bios.2020.112709.

[17] D. Najjar, J. Rainbow, S. Sharma Timilsina, P. Jolly, H. de Puig, M. Yafia, N. Durr, H. Sallum, G. Alter, J.Z. Li, X.G. Yu, D.R. Walt, J.A. Paradiso, P. Estrela, J.J. Collins, D.E. Ingber, A lab-on-a-chip for the concurrent electrochemical detection of SARS-CoV-2 RNA and anti-SARS-CoV-2 antibodies in saliva and plasma, Nat. Biomed. Eng. 6 (2022) 968–978, https://doi.org/10.1038/s41551-022-00919-w.

[18] A.R. Cardoso, J.F. Alves, M.F. Frasco, A.M. Piloto, V. Serrano, D. Mateus, A. I. Sebastião, A.M. Matos, A. Carmo, T. Cruz, E. Fortunato, M.G.F. Sales, An ultra-sensitive electrochemical biosensor using the Spike protein for capturing antibodies against SARS-CoV-2 in point-of-care, Mater. Today Bio 16 (2022), https://doi.org/10.1016/j.mtbio.2022.100354.

[19] L. Dai, D.W. Chang, J.B. Baek, W. Lu, Carbon nanomaterials for advanced energy conversion and storage, Small 8 (2012) 1130–1166, https://doi.org/10.1002/smll.201101594.

[20] A.C. Marques, A.R. Cardoso, R. Martins, M.G.F. Sales, E. Fortunato, Laser-induced graphene-based platforms for dual biorecognition of molecules, ACS Appl. Nano Mater. 3 (2020) 2795–2803, https://doi.org/10.1021/acsanm.0c00117.

[21] L. de Souza Freire, C.M. Ruzo, B.B. Salgado, A.M.D. Gandarilla, Y. Romaguera-Barcelay, A.P.M. Tavares, M.G.F. Sales, I. Cordeiro, J.D.B. Lalwani, R. Matos, H. Fonseca Filho, S. Astolfi-Filho, Ş. Ţălu, P. Lalwani, W.R. Brito, An electrochemical immunosensor based on carboxylated graphene/SPCE for IgG-SARS-CoV-2 nucleocapsid determination, Biosensors (Basel) 12 (2022), https://doi.org/10.3390/bios12121161.

[22] A.R. Cardoso, G. Cabral-Miranda, A. Reyes-Sandoval, M.F. Bachmann, M.G. F. Sales, Detecting circulating antibodies by controlled surface modification with specific target proteins: application to malaria, Biosens. Bioelectron. 91 (2017) 833–841, https://doi.org/10.1016/j.bios.2017.01.031.

[23] D.G. Papageorgiou, I.A. Kinloch, R.J. Young, Mechanical properties of graphene and graphene-based nanocomposites, Prog. Mater. Sci. 90 (2017) 75–127, https://doi.org/10.1016/j.pmatsci.2017.07.004.

[24] S.N. Korobeynikov, V.V. Alyokhin, A.V. Babichev, On the molecular mechanics of single layer graphene sheets, Int. J. Eng. Sci. 133 (2018) 109–131, https://doi.org/10.1016/j.ijengsci.2018.09.001.

[25] B. Gürünlü, Ç. Taşdelen-Yücedağ, M. Bayramoğlu, Graphene synthesis by ultrasound energy-assisted exfoliation of graphite in various solvents, Crystals 10 (2020), https://doi.org/10.3390/cryst10111037.

[26] L.P.T. Carneiro, A.M.F.R. Pinto, M.G.F. Sales, Development of an innovative flexible paper-based methanol fuel cell (PB-DMFC) sensing platform – application to sarcosine detection, Chem. Eng. J. 452 (2023), https://doi.org/10.1016/j.cej.2022.139563.

[27] A.V. Tyurnina, I. Tzanakis, J. Morton, J. Mi, K. Porfyrakis, B.M. Maciejewska, N. Grobert, D.G. Eskin, Ultrasonic exfoliation of graphene in water: a key parameter study, Carbon N Y 168 (2020) 737–747, https://doi.org/10.1016/j.carbon.2020.06.029.

[28] A. Amiri, M. Naraghi, G. Ahmadi, M. Soleymaniha, M. Shanbedi, A review on liquid-phase exfoliation for scalable production of pure graphene, wrinkled, crumpled and functionalized graphene and challenges, FlatChem 8 (2018) 40–71, https://doi.org/10.1016/j.flatc.2018.03.004.

[29] B. Gürünlü, Ç. Taşdelen-Yücedağ, M. Bayramoğlu, Graphene synthesis by ultrasound energy-assisted exfoliation of graphite in various solvents, Crystals (Basel) 10 (2020) 1–12, https://doi.org/10.3390/cryst10111037.

[30] F. Tuinstra, J.L. Koenig, Raman spectrum of graphite, J. Chem. Phys. 53 (1970) 1126–1130, https://doi.org/10.1063/1.1674108.

[31] N. Xiao, X. Dong, L. Song, D. Liu, Y. Tay, S. Wu, L.J. Li, Y. Zhao, T. Yu, H. Zhang, W. Huang, H.H. Hng, P.M. Ajayan, Q. Yan, Enhanced thermopower of graphene films with oxygen plasma treatment, ACS Nano 5 (2011) 2749–2755, https://doi.org/10.1021/nn2001849.

[32] S. Stankovich, D.A. Dikin, R.D. Piner, K.A. Kohlhaas, A. Kleinhammes, Y. Jia, Y. Wu, S.B.T. Nguyen, R.S. Ruoff, Synthesis of graphene-based nanosheets via chemical reduction of exfoliated graphite oxide, Carbon N Y 45 (2007) 1558–1565, https://doi.org/10.1016/j.carbon.2007.02.034.

[33] S. Ahadian, M. Estili, V.J. Surya, J. Ramón-Azcón, X. Liang, H. Shiku, M. Ramalingam, T. Matsue, Y. Sakka, H. Bae, K. Nakajima, Y. Kawazoe, A. Khademhosseini, Facile and green production of aqueous graphene dispersions for biomedical applications, Nanoscale 7 (2015) 6436–6443, https://doi.org/10.1039/c4nr07569b.

[34] A.F. Carvalho, T. Holz, N.F. Santos, M.C. Ferro, M.A. Martins, A.J.S. Fernandes, R. F. Silva, F.M. Costa, Simultaneous CVD synthesis of graphene-diamond hybrid films, Carbon N Y 98 (2016) 99–105, https://doi.org/10.1016/j.carbon.2015.10.095.

[35] A.C. Ferrari, D.M. Basko, Raman spectroscopy as a versatile tool for studying the properties of graphene, Nat. Nanotechnol. 8 (2013) 235–246, https://doi.org/10.1038/nnano.2013.46.

[36] W. Li, C. Tan, M.A. Lowe, H.D. Abruña, D.C. Ralph, Electrochemistry of individual monolayer graphene sheets, ACS Nano 5 (2011) 2264–2270, https://doi.org/10.1021/nn103537q.

[37] A.R. Cardoso, A.C. Marques, L. Santos, A.F. Carvalho, F.M. Costa, R. Martins, M.G. F. Sales, E. Fortunato, Molecularly-imprinted chloramphenicol sensor with laser-induced graphene electrodes, Biosens. Bioelectron. 124–125 (2019) 167–175, https://doi.org/10.1016/j.bios.2018.10.015.

[38] G. Martins, J.L. Gogola, L.H. Budni, M.A. Papi, M.A.T. Bom, M.L.T. Budel, E.M. de Souza, M. Müller-Santos, B.C.B. Beirão, C.E. Banks, L.H. Marcolino-Junior, M. F. Bergamini, Novel approach based on GQD-PHB as anchoring platform for the development of SARS-CoV-2 electrochemical immunosensor, Anal. Chim. Acta 1232 (2022), https://doi.org/10.1016/j.aca.2022.340442.

[39] B.A. Braz, M. Hospinal-Santiani, G. Martins, C.S. Pinto, A.J.G. Zarbin, B.C. B. Beirão, V. Thomaz-Soccol, M.F. Bergamini, L.H. Marcolino-Junior, C.R. Soccol, Graphene-binding peptide in fusion with SARS-CoV-2 antigen for electrochemical immunosensor construction, Biosensors (Basel) 12 (2022), https://doi.org/10.3390/bios12100885.